



## Space geodetic determination of spatial variability in relative sea level change, Los Angeles basin

B. A. Brooks,<sup>1</sup> M. A. Merrifield,<sup>2</sup> J. Foster,<sup>1</sup> C. L. Werner,<sup>3</sup> F. Gomez<sup>4</sup>  
M. Bevis,<sup>5</sup> and S. Gill<sup>6</sup>

Received 13 September 2006; revised 2 November 2006; accepted 21 November 2006; published 12 January 2007.

[1] We combine Synthetic Aperture Radar Interferometry (InSAR), tide gauge, and continuous GPS measurements to determine the spatial variation in vertical land motion (VLM) along the coast of the Los Angeles basin over the past decade, and to examine the impact of spatially variable VLM on relative sea level trends. By identifying radar scattering targets with long-term coherence we make height corrections which allow interferogram creation for nearly the entire ERS-1 catalog and permit estimation of average deformation rates with minimal temporal aliasing. Between Los Angeles Harbor and Newport Beach, mean VLM trends range from  $\sim 3.4$  to  $-4.3$  mm/yr, reflecting the high level of ground water and oil extraction activity in the region. West of Los Angeles Harbor, VLM rates and spatial variability are roughly half as large. The 8-year VLM trends exceed the long-term sea level trend (0.8 mm/yr) determined from the 80 year Los Angeles Harbor tide gauge. The high degree of observed VLM variability emphasizes the need for the spatially continuous measurements provided by InSAR; a single tide gauge assessment of regional RSL would otherwise have limited applicability. **Citation:** Brooks, B. A., M. A. Merrifield, J. Foster, C. L. Werner, F. Gomez, M. Bevis, and S. Gill (2007), Space geodetic determination of spatial variability in relative sea level change, Los Angeles basin, *Geophys. Res. Lett.*, 34, L01611, doi:10.1029/2006GL028171.

### 1. Introduction

[2] Mitigating the effects of sea level rise is a major societal challenge for the 21st century. Recent satellite altimeter observations indicate that the rate of global sea level (GSL) rise is  $\sim 3$  mm/yr since the mid-1990s [Leuliette *et al.*, 2004], an increase above the 1–2 mm/yr 20th century rate determined from tide gauges (see summary in Church *et al.* [2001]). This apparent acceleration heightens concerns not only of the pace of shoreline encroachment, but also of the damaging impacts of extreme water level events

associated with high waves and storms that are expected to increase as coastal sea levels rise. Accurate assessment of sea level rates therefore is an important concern for coastal managers and policy makers concerned with the protection of lives and property along the coast.

[3] Local determination of the rate of change of relative sea level (RSL), or the water level relative to the adjacent land, is likely to differ considerably from the GSL rate, which is referenced ideally to the earth's center of mass or geoid. This is due in part to ocean variability, which leads to decadal and longer period fluctuations that dominate RSL rates at these time scales [Douglas, 2001]. Even if sufficient data are available to differentiate secular trends from ocean variability, vertical land motion (VLM) can contribute to RSL trends at a level comparable to the ocean. A prominent contributor to VLM is the rebound of the continents associated with the reduction in land ice mass following the last ice age, or post-glacial rebound (PGR). RSL measured along many high latitude coasts is falling over time [Woodworth, 1990] and direct GPS measurements have been used to confirm the PGR contribution [Scherneck *et al.*, 2001]. PGR is a geologic time scale phenomenon that appears as a secular trend component in tide gauge observations. Models have been developed to estimate PGR rates [Tushingham and Peltier, 1991], which are important primarily for high latitude locations.

[4] At mid- to low-latitudes, other processes tend to dominate the coastal VLM signals. Local deformations due to ground water or oil extraction, the settling of landfill, and earthquakes and other tectonic effects are likely to have short spatial scales and nonlinear and abrupt behavior in time; consequently they are much more difficult to model than PGR. A single VLM measurement at an unstable location is unlikely to represent motion over a larger area, unlike a PGR-dominated site.

[5] Continuous GPS (CGPS) measurements at tide gauges and/or tide gauge benchmarks provides a means of correcting for VLM signals in sea level records [Bevis *et al.*, 2002; Mitchum, 1998]. This allows for an estimate of VLM at the tide gauge, but not of the surrounding region. Dense CGPS networks such as the Southern California Integrated GPS Network (SCIGN) can provide information on regional relative ground motion; however, even a network as extensive as SCIGN is essentially a collection of point measurements that are sparse relative to VLM spatial scales and along the coast where information is needed in determining RSL (Figure 1).

[6] Here, we demonstrate how the emerging technique of satellite-based InSAR [Burgmann *et al.*, 2000] combined with traditional tide gauge observations, can provide RSL estimates for a coastal region with unprecedented spatial

<sup>1</sup>Hawaii Institute of Geophysics and Planetology, School of Ocean and Earth Science and Technology, University of Hawaii, Honolulu, Hawaii, USA.

<sup>2</sup>Department of Oceanography, School of Ocean and Earth Science and Technology, University of Hawaii, Honolulu, Hawaii, USA.

<sup>3</sup>Gamma Remote Sensing Research and Consulting AG, Gumligen, Switzerland.

<sup>4</sup>Department of Geological Sciences, University of Missouri, Columbia, Missouri, USA.

<sup>5</sup>Geodetic Science, Ohio State University, Columbus, Ohio, USA.

<sup>6</sup>Center for Operational Oceanographic Products and Services, NOAA, Silver Spring, Maryland, USA.

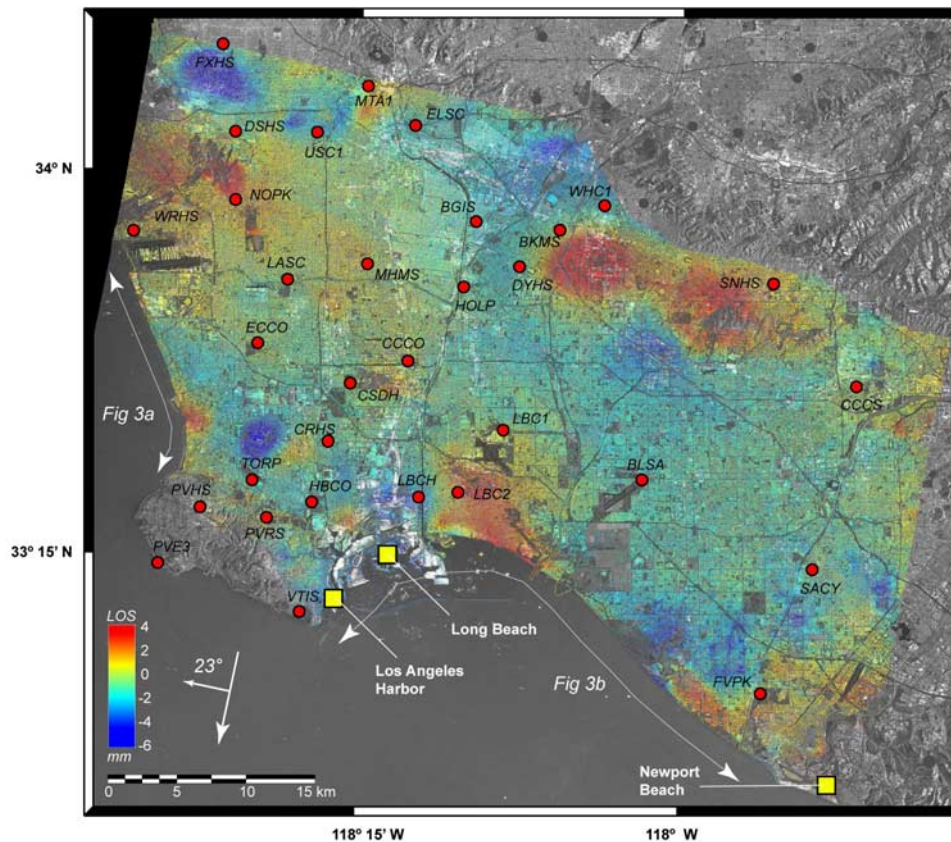


**Figure 1.** Linear line of sight (LOS) velocity from 1992–2000 from ERS-1 descending passes. Continuous GPS stations from the SCIGN network used in our analysis (red circles), NOS tide gauge stations (yellow squares). LOS velocity is with respect to GPS station PVRS. Double-arrow lines along coast indicate areas for the coastal strips plotted in Figure 3. Legend arrow shows ERS LOS azimuth and inclination ( $23^\circ$ ).

resolution. For the Los Angeles basin region we produce a map of VLM rates from 1992–2000 with horizontal resolution of 20 meters and vertical resolution of a few millimeters. Previous studies have produced similar results although they were focused primarily on characterizing the tectonic and anthropogenic deformation signal throughout the region [Argus *et al.*, 2005; Bawden *et al.*, 2001; Lanari *et al.*, 2004]; here we focus on the coastal signal. The map allows us to estimate VLM in the immediate vicinity of a centrally located tide gauge and yields a regional assessment of RSL for two continuous coastal strips of  $\sim 15$  and 45 km length.

## 2. Mapping Land Motion: InSAR Processing and Results

[7] Applying InSAR for space-based deformation mapping of sub-cm scale signals has been reviewed extensively by other authors [Burgmann *et al.*, 2000; Hanssen, 2001; Rosen *et al.*, 2000]. InSAR measures the earth surface displacement field along the radar's line-of-sight (LOS, for ERS-1/2 satellites  $\sim 23^\circ$  from vertical) by interfering and phase-differencing of time-separated images and removal of the topographic phase with a digital elevation model (DEM). The technique is limited by the degree of interferometric coherence for targets on the ground between acquisitions. In addition to temporal [Rosen *et al.*, 2000;

Zebker and Villasenor, 1992] and seasonal decorrelation [Lu and Freymueller, 1998; Wicks *et al.*, 1998], geometrical baseline decorrelation for distributed scattering targets is proportional to the component of the baseline perpendicular to the line of sight. Because the combination of path length difference along the line of sight due to deformation, variations in atmospheric path delay, and noise generally exceed half a wavelength, the interferometric phase must be unwrapped to resolve spatial and temporal ambiguities [Goldstein *et al.*, 1988].

[8] Recently developed processing utilizes the fact that for stable, point-like reflectors, minimal baseline-related decorrelation occurs and so interferometric phase may be interpreted even for data pairs with long perpendicular baselines that may exceed the critical baseline [Dixon *et al.*, 2006; Ferretti *et al.*, 2001; Hooper *et al.*, 2004; Werner *et al.*, 2003]. This general class of 'persistent scatterer' techniques is especially useful in urban areas where a large number of suitable scatterers can be found. For this study of the Los Angeles basin area we processed 59 ERS-1 descending interferograms spanning  $\sim 8$  years from 1992–2000 (track 170, frame 2925) using GAMMA software and the persistent scatterer technique of Werner *et al.* [2003]. This is different than previous studies that used the same data set but with more traditional processing that did not include the determination of individual scattering targets

[Argus *et al.*, 2005; Bawden *et al.*, 2001; Lanari *et al.*, 2004].

[9] We determined point targets using joint measures of backscatter temporal amplitude variability and spatial spectral diversity of candidate points. The amplitude measure is defined as the ratio of the mean and standard deviation of backscatter intensity for each point in a temporal data stack [Ferretti *et al.*, 2001]. The spatial spectral diversity is determined by first calculating the spectrum in a  $4 \times 4$  region about each pixel. The 2-D spectrum is divided into individual looks and the look statistics are evaluated: low intensity variation for the individual looks indicates point-like scattering.

[10] With candidate point targets selected we generated differential interferograms for each scene using a common reference scene (Jan. 11, 1997; see auxiliary material<sup>1</sup> for scene list). At this stage, many of the image pairs with larger perpendicular baselines demonstrated high enough levels of phase noise to preclude their use for analysis. To mitigate this, for each point and time period in the data volume, we linearly regressed phase versus perpendicular baseline in order to extract height corrections due to the linear relationship between perpendicular baseline and topographic phase dictated by SAR imaging geometry [Hanssen, 2001]. Simultaneously, we also regressed for linear deformation rate at each pixel so that the height corrections would not be contaminated by any deformation signal. The first part of the regression allowed for pointwise height correction of the original DEM (we used the USGS 10 meter DEM) and recalculation of the differential interferograms resulting in an increased number of scenes with interpretable phase data. We note that in this single reference image approach, some baselines will be very large. It is for these large baselines that the point scatterers are essential because they do not exhibit geometric baseline decorrelation. Precisely because the baseline is large, however, determination of point heights are needed to adequately remove topographic phase. Indeed, in urban areas, the scatterer height can differ by 10s of meters from the DEM height because the scatterer may be the roof of a building.

[11] After spatially unwrapping each interferogram using a minimum cost flow algorithm [Chen and Zebker, 2000], we refined baseline estimates and regenerated the differential interferograms. We iterated the regression process 3 times, discarding low quality points, until essentially the entire catalog produced interferograms with interpretable phase for use in estimating a linear deformation rate that is not temporally aliased (Figure 1). This is especially important in an area such as the Los Angeles basin which exhibits strong seasonal deformation variation [Argus *et al.*, 2005; Bawden *et al.*, 2001; Lanari *et al.*, 2004].

[12] The residual phase includes both non-linear deformation and atmospheric components. For our study area Lanari *et al.* [2004] and Argus *et al.* [2005] showed that non-linear deformation can have an amplitude on the order of 10s of mms over time-scales as short as years. However, because our goal is to compare with longer-term ( $\sim$ decadal) tide gauge records, the non-linear deformation component is of second-order importance. This is further corroborated by

<sup>1</sup>Auxiliary materials are available at <ftp://ftp.agu.org/apend/g/l/2006gl028171>.

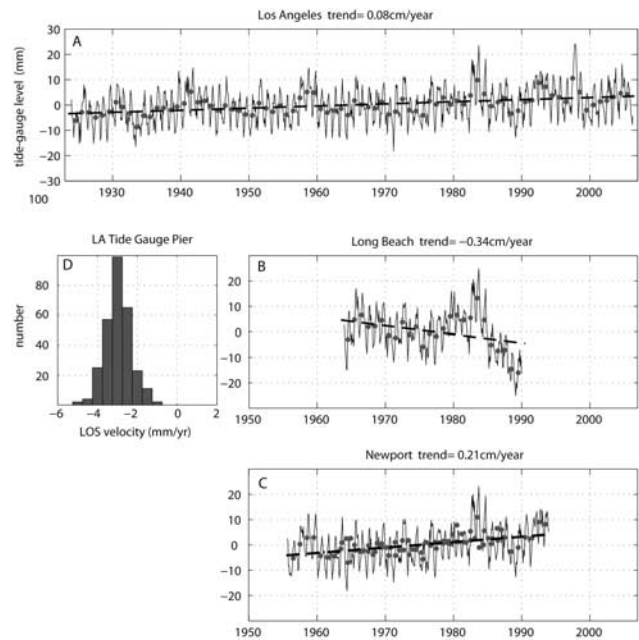


**Figure 2.** Tide gauge records and long-term linear trends from stations in Figure 1. (a) Los Angeles, (b) Long Beach, (c) Newport, and (d) histogram of LOS velocity determined for the pier where the Los Angeles tide gauge and benchmarks reside.

Lanari *et al.* [2004] who found that the coastal areas focused on in our study exhibit very low correlation with the strong seasonal oscillations associated with the Santa Ana aquifer [Lanari *et al.*, 2004, Figure 4a]. Additionally, because atmospheric water vapor does not exhibit temporal correlation over time-scales as long as the ERS-1 35 day repeat cycle, its contribution to the final result should be effectively mitigated by the linear regression with respect to time.

[13] Our resulting LOS deformation rate estimates (Figure 1) are similar to previously published results using the same data sets but different processing techniques [Argus *et al.*, 2005; Bawden *et al.*, 2001; Lanari *et al.*, 2004]. Large local relative deformations on the order of  $\sim 1$  cm/yr are observed associated with oil and water withdrawal and recharge [Argus *et al.*, 2005; Bawden *et al.*, 2001; Lanari *et al.*, 2004].

### 3. Relative Sea-Level Change

[14] The National Ocean Service (NOS) NOAA currently operates two tide gauges in the greater Los Angeles area at Los Angeles Outer Harbor, and Santa Monica Pier (because the Santa Monica site falls to the northwest of our ERS-1 scene boundary we do not analyze it here). Two historical long-term NOAA tide stations at Newport Beach Harbor and Long Beach Harbor provide data for this study but are no longer in operation. (Figure 1, auxiliary material Table S1). NOS periodically publishes RSL trends from the NOAA National Water Level Observation Network (NWLON) [Zervas, 2001]. The record at Los Angeles is uninterrupted since 1923 (Figure 2a). The Long Beach station was in operation from 1964 – 1990, however it was discontinued

by NOAA in 1990 because the tidal signal was redundant with the nearby station at Los Angeles Outer Harbor and because the extreme rates of differential land movement among the bench marks made it impossible to compute a reference datum for navigation purposes (Figure 2b). Newport Harbor is the only other station in the region with a record at least 10 years long (1955 to 1994, Figure 2c). The RSL time series show considerable interannual variability that is common to the various sites, particularly the high water levels associated with major El Nino events. Superposed on the variable RSL is a linear trend that varies at each site. Over the duration of their individual record lengths, linear RSL trends range from  $-3.4$  mm/yr at Long Beach to  $2.17$  mm/yr at Newport Beach (Figure 2, auxiliary material Table S1), all significantly different than zero at the 95% confidence level assuming an integral time scale of two years for each station. The RSL rise from the longest record at Los Angeles is  $0.82 \pm 0.23$  mm/yr, which is about one-half the GSL rate estimated in various tide gauge studies [e.g., Douglas, 2001]. We interpret the variations in these rates between stations over the common time period, particularly the  $\sim 1.0$  mm/yr difference between Newport and Los Angeles as an indication of different VLM rates at the two stations (i.e., over 38 year time periods we assume that the ocean contribution to the trends is similar at these stations separated by 50 km or less). For the time period when InSAR rates are computed (1992–2000), sea level has been dropping at a fast rate at Los Angeles (auxiliary material Table S1). This is due to decadal variations in sea level, which have caused falling rates recently along the west coast of North America [Firing *et al.*, 2004].

[15] The Long Beach record is an example of a tide gauge that is clearly affected by anomalous land motions. A positive VLM rate (in contrast to the InSAR measured rates here) presumably causes the drastic fall in sea level over the 26 year record length, which is anomalous behavior compared to the other tide gauges. We note also that the downward trend is not steady over time, with some episodic jumps leading to a fast decline over the latter part of the record. It was the unstable nature of this tide gauge station that led NOS to decommission the site. For the purposes of this study, the Long Beach record confirms that strong and nonlinear VLM signals occur along this coast.

[16] Based on the limited number of Los Angeles area tide gauges records available, it is evident that estimated trends vary both spatially and temporally, with different time segments yielding different rates. Here, we focus on the long Los Angeles Harbor tide gauge because it is the longest continuous record, and because the tide gauge and its benchmarks are located within our InSAR deformation map (Figure 1).

[17] To convert the Los Angeles tide gauge RSL trend ( $b_{LA} = 0.82$  mm/yr) to the RSL trend at other locations along the coast ( $b(x)$ ), we first compute the VLM trend at the Los Angeles tide gauge benchmarks ( $L_{LA}$ ) as the median InSAR vertical displacement for the entire pier where the tide gauge and benchmarks reside (Figure 2d). We use the convention that a negative VLM rate corresponds to a net downward displacement over time. The InSAR vertical displacement rate at other locations along the coast ( $L(x)$ ) is then

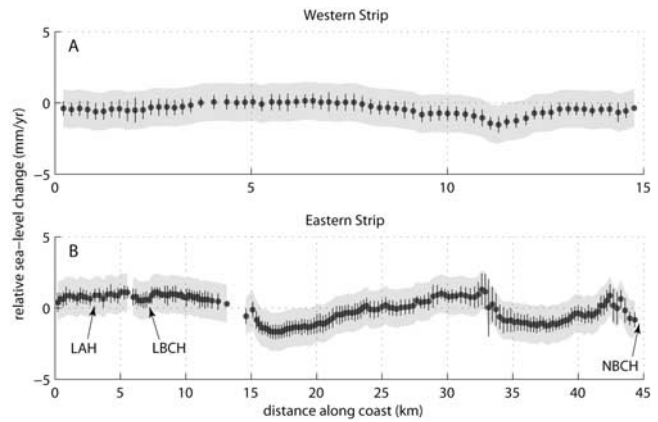


**Figure 3.** Profiles of relative sea-level change referenced to the Los Angeles Harbor tide gauge. (a) Profile west of Palos Verdes, and (b) profile east of Palos Verdes. Profiles are formed by taking the mean value in a 100 m wide (along the coast) by 500 m long (perpendicular to the coast) rectangle, spaced every 250 m along the strip. LAH, the location of Los Angeles Harbor tide gauge; LBCH, Long Beach tide gauge; and NBCH, Newport Beach tide gauge. Grey shading indicates  $2\sigma$  errors determined from the maximum horizontal motions of the CGPS stations (see text for discussion). Black lines show  $2\sigma$  values from each rectangle in the strip.

subtracted from the sum of  $b_{LA}$  and  $L_{LA}$ , which gives the RSL trend along the coast,

$$b(x) = b_{LA} + L_{LA} - L(x).$$

[18] We examine two strips on either side of the Palos Verde peninsula and estimate RSL along the coast by taking the mean value in a 100 m wide (along the coast) by 500 m long (perpendicular to the coast) rectangle, spaced every 250 m along the strip (Figure 3). The western strip, which extends from Vista del Mar to the northwestern margin of the Palos Verde peninsula, shows very little indication of an RSL rise. Median trends range from  $0.1$  to  $-1.5$  mm/yr with the majority of the values less than zero. Along the eastern strip, extending from the eastern margin of the Palos Verde peninsula to Newport Beach, the rates are much more variable ranging from a low of  $-1.7$  mm/yr in the vicinity of Long Beach, to a high of  $1.3$  mm/yr in the vicinity of Huntington Beach. These results suggest that in either of these regions, simply using the Los Angeles Harbor tide gauge alone would provide a poor indication of RSL trends – for the western strip the sign of RSL change everywhere would be reversed, and for the eastern strip, the spatial variability as well as RSL sign would not be represented.

[19] Because InSAR in a single look direction records only one displacement, it is possible that horizontal motion could contribute to LOS observations and so contaminate VLM estimates. For ERS-1 the effect should be small because the satellite has an incidence angle inclined  $23^\circ$  from vertical; nonetheless, because of the LA basin's well-known differential tectonic signals we evaluate horizontal velocity contributions using the wide-spread SCIGN CGPS

network (Figure 1). For the time period of the InSAR data, we use velocity solutions from 30 SCIGN stations (<http://sopac.ucsd.edu/>) and find a reference frame via a 6 parameter Helmert transformation (3 rotations, 3 rotation rates) in which horizontal velocities are minimized in a least-squares sense. So as to compare most appropriately with InSAR, we use velocity solutions that do not have seasonal signals removed. The frame we find has residual rms velocities less than  $\sim 2.6$  mm/yr and effectively places the CGPS site velocities in the same reference frame as the InSAR data. We estimate a maximum horizontal contribution to InSAR-determined VLM of  $\pm 1.2$  mm/yr by taking the residual  $2\sigma$  horizontal velocity magnitude (3.1 mm/yr) and projecting it onto LOS and then onto vertical (Figure 3). This estimate is overly conservative, however, because very few of the residual vectors are aligned in the LOS direction, and so the spatial scatter exhibited in each rectangle along the strip is a more realistic error indicator (Figure 3).

#### 4. Discussion

[20] The combined InSAR, CGPS, and tide gauge method shows that RSL changes can occur with positive or negative magnitudes on short spatial scales ( $<10$  km) along the coast of the Los Angeles basin. The strip between Los Angeles Harbor and Newport Beach exhibits the highest variability in RSL trend, consistent with the aforementioned ground water and oil extraction and recharge in the region [Argus et al., 2005; Bawden et al., 2001; Lanari et al., 2004]. The high VLM variability in this region is also consistent with the irregular Long Beach tide gauge record.

[21] We caution that the InSAR and CGPS datasets are still relatively short ( $\sim 10$  years) compared to the tide gauge record ( $>80$  years), which introduces uncertainty as to how representative the recent VLM estimates are of long-term land motion at the tide gauge. This is particularly a concern for tectonically and anthropogenically active areas like the LA basin where abrupt seismic events and intensive coastal land use practices introduce complicated VLM signals that are not well-modeled by a linear trend computed over decade long records. The same is true, however, for VLM estimates based on similarly short CGPS time series. Longer InSAR records are needed to assess the dominant spatio-temporal scales of VLM motion over this region, which will allow for more conclusive integrations of tide gauge and CGPS measurements. In order for long-term InSAR time series to be created it will be important to further develop persistent scatterer techniques such as used in this and other studies [Dixon et al., 2006; Ferretti et al., 2001; Hooper et al., 2004; Werner et al., 2003]. Importantly, the high degree of observed VLM variability emphasizes the need for the spatially continuous measurements provided by InSAR; a single tide gauge assessment of regional RSL would otherwise have limited applicability.

[22] This joint analysis provides a new type of tool for coastal scientists and managers interested in detailed quantification of RSL for a region. For instance, Zhang et al. [2004] suggest that there is a multiplicative relationship between long-term sandy beach erosion and sea-level rise that is well-approximated by the 'Bruun rule' – a simple geometric expression that predicts a linear relationship between coastal retreat and sea-level rise assuming beaches

trend towards an equilibrium profile. Our findings raise the possibility that differences in shoreline rates of change along the Southern California coast may be due in part to spatially varying RSL. InSAR-produced RSL maps could yield deeper physical understanding and predictive power of beach morphology evolution.

[23] Finally, not only can RSL be estimated directly, but also the contribution of land motion to RSL can be estimated using a combination of CGPS and InSAR data. When absolute vertical rates can be established using a CGPS network properly referenced to a global datum, the InSAR maps would provide the leveling tie between the CGPS stations and the tide gauge benchmarks, thus allowing for an absolute land correction at the tide gauge. In this way, ocean rates can be estimated from the tide gauge for comparison with distant tide gauge stations that are also linked via CGPS, as well as with satellite altimeters that are in the same frame of reference.

[24] **Acknowledgments.** Support for this study was provided by NASA. We thank G. Pawlak and C. Fletcher for helpful discussion. We thank Donald Argus and an anonymous reviewer for suggestions which improved the manuscript. ERS-1 data courtesy of the WINSAR archive. SOEST contribution 7013.

#### References

- Argus, D. F., M. B. Heflin, G. Peltzer, F. Crampé, and F. H. Webb (2005), Interseismic strain accumulation and anthropogenic motion in metropolitan Los Angeles, *J. Geophys. Res.*, *110*, B04401, doi:10.1029/2003JB002934.
- Bawden, G. W., et al. (2001), Tectonic contraction across Los Angeles after removal of groundwater pumping effects, *Nature*, *412*, 812–815.
- Bevis, M., et al. (2002), Technical issues and recommendations related to the installation of continuous GPS stations at tide gauges, *Mar. Geod.*, *25*, 87–99.
- Burgmann, R., et al. (2000), Synthetic aperture radar interferometry to measure Earth's surface topography and its deformation, *Annu. Rev. Earth Planet. Sci.*, *28*, 169–209.
- Chen, C., and H. Zebker (2000), Network approaches to two-dimensional phase unwrapping: Intractability and two new algorithms, *J. Opt. Soc. Am. A Opt. Image Sci.*, *17*, 401–414.
- Church, J., et al. (2001), Changes in sea level, in *Climate Change 2001: The Scientific Basis: Contribution of Working Group I to the Third Assessment Report of the Intergovernmental Panel on Climate Change*, edited by J. Houghton et al., pp. 639–694, Cambridge Univ. Press, New York.
- Dixon, T. H., et al. (2006), Subsidence and flooding in New Orleans, *Nature*, *441*, 587–588.
- Douglas, B. (2001), Sea level changes in the era of the recording tide gauge, in *Sea Level Rise: History and Consequences*, edited by B. Douglas et al., pp. 37–64, Elsevier, New York.
- Ferretti, A., et al. (2001), Permanent scatterers in SAR interferometry, *IEEE Trans. Geosci. Remote Sens.*, *39*, 8–20.
- Firing, Y. L., et al. (2004), Interdecadal sea level fluctuations at Hawaii, *J. Phys. Oceanogr.*, *34*, 2514–2524.
- Goldstein, R. M., et al. (1988), Satellite radar interferometry: Two-dimensional phase unwrapping, *Radio Sci.*, *23*, 713–720.
- Hanssen, R. F. (2001), *Radar Interferometry: Data Interpretation and Error Analysis*, 308 pp., Springer, New York.
- Hooper, A., H. Zebker, P. Segall, and B. Kampes (2004), A new method for measuring deformation on volcanoes and other natural terrains using InSAR persistent scatterers, *Geophys. Res. Lett.*, *31*, L23611, doi:10.1029/2004GL021737.
- Lanari, R., P. Lundgren, M. Manzo, and F. Casu (2004), Satellite radar interferometry time series analysis of surface deformation for Los Angeles, California, *Geophys. Res. Lett.*, *31*, L23613, doi:10.1029/2004GL021294.
- Leuliette, E. W., et al. (2004), Calibration of TOPEX/Poseidon and Jason altimeter data to construct a continuous record of mean sea level change, *Mar. Geod.*, *27*, 79–94.
- Lu, Z., and J. T. Freymueller (1998), Synthetic aperture radar interferometry coherence analysis over Katmai volcano group, Alaska, *J. Geophys. Res.*, *103*, 29,887–29,894.

- Mitchum, G. T. (1998), Monitoring the stability of satellite altimeters with tide gauges, *J. Atmos. Oceanic Technol.*, *15*, 721–730.
- Rosen, P. A., S. Henseley, I. R. Joughin, F. K. Li, S. N. Madsen, E. Rodriguez, and R. M. Goldstein (2000), Synthetic aperture radar interferometry, *Proc. IEEE*, *88*, 333–382.
- Scherneck, H.-G., et al. (2001), BIFROST project: 3-D crustal deformation rates derived from GPS confirm postglacial rebound in Fennoscandia, *Earth Planets Space*, *53*, 703–708.
- Tushingham, A. M., and W. R. Peltier (1991), Ice-3G: A new global model of late Pleistocene deglaciation based upon geophysical predictions of post-glacial relative sea level change, *J. Geophys. Res.*, *96*, 4497–4523.
- Werner, C., et al. (2003), Interferometric point target analysis with JERS-1 L-band SAR data, paper presented at International Geoscience and Remote Sensing Symposium, Inst. of Electr. and Electron. Eng., Toulouse, France, 21–25 Jul.
- Wicks, C. W., Jr., et al. (1998), Migration of fluids beneath Yellowstone Caldera inferred from satellite radar interferometry, *Science*, *282*, 458–462.
- Woodworth, P. (1990), A search for accelerations in records of European mean sea level, *Int. J. Climatol.*, *10*, 129–143.
- Zebker, H. A., and J. Villasenor (1992), Decorrelation in interferometric radar echoes, *IEEE Trans. Geosci. Remote Sens.*, *30*, 950–959.
- Zervas, C. (2001), Sea level variations of the United States 1854–1999, *Tech. Rep. NOS CO-OPS 36*, 186 pp., NOAA Cent. for Oper. Oceanogr. Prod. and Serv., Silver Spring, Md.
- 
- M. Bevis, Geodetic Science, Ohio State University, 2036 Neil Avenue, Columbus, OH 43210, USA.
- B. A. Brooks and J. Foster, Hawaii Institute of Geophysics and Planetology, SOEST, University of Hawaii, 1680 East-West Road, Honolulu, HI 96822, USA. (bbrooks@soest.hawaii.edu)
- S. Gill, Center for Operational Oceanographic Products and Services, NOAA, Silver Spring, MD 20910, USA.
- F. Gomez, Department of Geological Sciences, University of Missouri, 101 Geology Building, Columbia, MO 65211, USA.
- M. A. Merrifield, Department of Oceanography, SOEST, University of Hawaii, 1680 East-West Road, Honolulu, HI 96822, USA.
- C. L. Werner, Gamma Remote Sensing Research and Consulting AG, Worbstrasse 225, CH-3073 Gumligen, Switzerland.